Geophysical Research Letters

RESEARCH LETTER
10.1029/2020GL088521

Strain Signals Before and During Paroxysmal Activity at Stromboli Volcano, Italy

Bellina Di Lieto[1], Pierdomenico Romano[1], Roberto Scarpa[2], and Alan Trevor Linde[3]

[1]Osservatorio Vesuviano, Istituto Nazionale di Geofisica e Vulcanologia, Naples, Italy, [2]Dipartimento di Fisica, Università di Salerno, Salerno, Italy, [3]Earth and Planets Laboratory, Carnegie Institution for Science, Washington, DC, USA

Key Points:
- Borehole dilatometers are widely used to monitor open- and closed-conduits volcanoes, recording areal strain changes due to volcanic sources
- A dilatometer recorded strain changes minutes before eruptions onset for 2019 activity: Correlation with 2007 paroxysm suggests common source
- For the first time a comparison high-frequency, high-sensitivity strain data for the 2007 and both 2019 vulcanian explosions are presented

Supporting Information:
- Supporting Information S1
- Data Set S1
- Data Set S2
- Figure S1
- Figure S2
- Figure S3
- Figure S4

Correspondence to:
P. Romano,
pierdomenico.romano@ingv.it

Citation:
Di Lieto, B., Romano, P., Scarpa, R., & Linde, A. T. (2020). Strain signals before and during paroxysmal activity at Stromboli volcano, Italy. *Geophysical Research Letters*, *47*, e2020GL088521. https://doi.org/10.1029/2020GL088521

Received 24 APR 2020
Accepted 21 SEP 2020
Accepted article online 28 SEP 2020

Author Contributions:
Formal analysis: Bellina Di Lieto, Pierdomenico Romano
Writing – original draft: Roberto Scarpa
Writing – review & editing: Alan Trevor Linde

Abstract In the last decades, Mt. Stromboli produced four vulcanian eruptions, in 2003 and 2007 and July and August 2019, recorded by INGV monitoring network. Specifically, last three events are studied through records from borehole strainmeters, which allow to infer details on source dynamics. These events are preceded by a slow strain buildup, starting several minutes before the paroxysms, which can be used in future for early warning. Eruptions consist of two or more strain pulses, with oscillations ranging from several seconds, as in 2007, to some minutes, as in 2019, and lasting from several minutes to 1 hr after the explosions.

Plain Language Summary Sacks-Evertson borehole dilatometers are a special kind of strainmeter, capable of recording volumetric strain changes. In the current manuscript, data recorded by such an instrument reveal that strain changes occurred several minutes before two paroxysmal events occurred in the summer of 2019 at Stromboli, an open-conduit volcano located in Eolian Islands, Italy. A comparison of 2019 paroxysms has been made with previous eruptions at Stromboli volcano: Similarities among the explosions suggest a common source mechanism. Starting from these observations, a real-time early warning system could be developed in the future, allowing Italian Civil Protection Department to set up automated (or semi-automated) variable alert levels, which could trigger alarms accordingly. Such an early warning system could then be used to provide alerts for other similar open-conduit volcanoes.

1. Foreword

Stromboli can be considered one of the most active volcanoes in the world. Its persistent but moderate explosive activity, termed "Strombolian," is interrupted by occasional episodes of more vigorous activity accompanied by lava flows, as seen in 1975, 1985, 2002–2003, 2007, 2014, and more recently in July and August 2019. Persistent eruptive activity and ease of access make this volcano an ideal laboratory for detailed study of source processes associated with magmatic activity.

The dynamics of the sources associated with the explosions has been investigated by Chouet et al. (1997, 1999, 2003) by using seismic arrays and a dense network of broadband seismometers. These authors investigated the very-long period (VLPs) source mechanisms, revealing a volumetric component attributed to mass transport through the magma conduits. Long period components of volcanic tremor (10–50 s) have been also documented (De Lauro et al., 2005; De Martino et al., 2005). The volcanic tremor of Stromboli is a continuous permanent signal with a spectrum covering traditionally a 1–3 Hz band. Just after the 2002 extensive phase of activity, the latter studies indicated the need to complement the monitoring system with some borehole strainmeters, instruments capable of recording the volcano behavior at low frequencies. Two such instruments were installed during 2006, with the support of Italian Civil Protection Department, by INGV, Università degli Studi di Salerno (Italy) and Carnegie Institution of Washington DC (USA): the TDF instrument, located near the Ginostra village in the western side of the island, lying at a radial distance of 1.5 km from the main eruptive vents, and the SVO instrument, situated in the village of Stromboli, about 2.5 km northeast from the summit craters (Figure 1).

The Sacks-Evertson strainmeters are long stainless steel cylinders of about 7 cm in diameter and 4 m in length filled with degassed silicone oil, which provide two signal outputs, obtained by two different hydro-mechanical amplification systems: A bigger sensing volume is connected with a small bellow, whose length changes in proportion to the volume of oil entering or leaving it. The position of the top of the bellow is measured through a linear variable differential transformer (LVDT). The dynamic range of the instrument is about 140 dB. A second, less sensitive, bellows-displacement transducer-valve assembly is connected with the

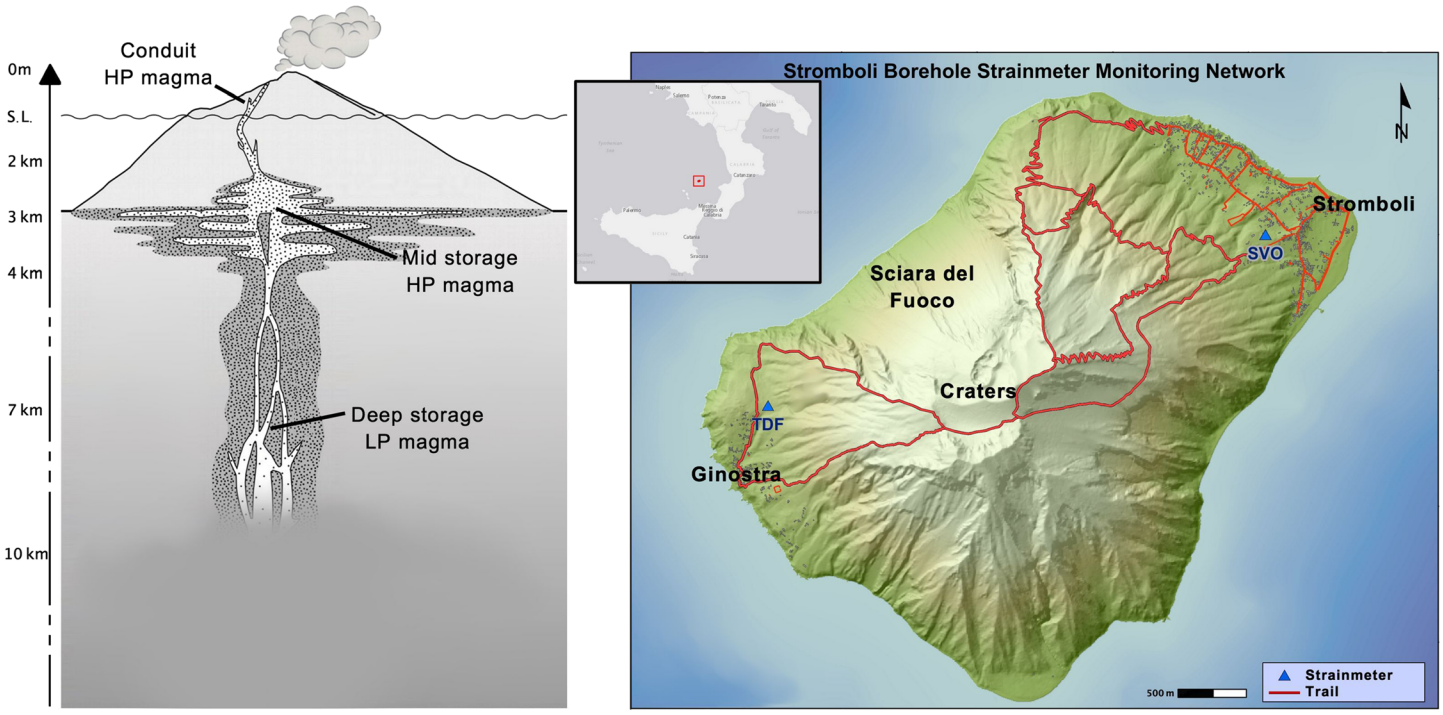

Figure 1. (left) Schematic possible model of the plumbing system (modified after Calvari et al., 2011; Métrich et al., 2010). (right) Location of Stromboli Island and of the two dilatometers.

first one. The high-sensitivity output integrates the volumetric change in the strained reservoir. The low-sensitivity one is connected to the strained reservoir only when the instrument is sensing a rapid and strong strain change, thus measuring strain. Usually, the low-sensitivity channel measures the pressure in a closed cell, that is proportional to local temperature. The temperature resolution is ~10 microdegrees. Air pressure is also measured. Nominal resolution of the Sacks-Evertson strainmeter is about 10^{-11}, nominal dynamic range is 10^{-11}–10^{-3}. Low-frequency calibration of installed strainmeters is obtained by comparison with Earth tides (Hart et al., 1996). Seismic signal, high- and low-sensitivity strain signals are continuously recorded and sampled at 50 sps. Sacks-Evertson strainmeters are installed in boreholes by using expansive cement to couple them to the surrounding rocks. Once installed, the strainmeters are not adjustable nor recoverable.

The two instruments installed in Stromboli are each cemented at the bottom of a borehole at 120 m depth. Data recorded at both sites are sent to Vesuvius Observatory and are retrieved and processed at Vesuvius Observatory and University of Salerno. After the installation, comparison of data from both strainmeters for low- and high-frequency signals (earth tides and summit explosions, respectively) revealed that the TDF instrument is not well coupled with the surrounding rocks, while the second (SVO) shows a sensitivity 1×10^{-11} per digital count.

In order to obtain the change in rock strain, data are processed by removing atmospheric pressure, Earth tides, and ocean loading by using a Bayesian approach (Hart et al., 1996).

Here we show a correlation among the previous paroxysmal eruption that occurred in 2007 and those during summer 2019: The strainmeter data show time-histories that are similar for all recorded paroxysms. This observation suggests a common source mechanism.

2. Paroxysms Comparison

2.1. The 2007 Paroxysm

Initial technical and logistic issues delayed the start of reliable continuous data recording until 20 January 2007. After a few weeks, an extensive phase of activity of the volcano, with a lava flow outpouring from

the northern flank, started at 1:30 p.m. on 27 February 2007 and a small vulcanian explosion occurred on 15 March 2007. This activity produced an ash column reaching a height of 3–3.5 km above the craters. The paroxysmal activity lasted about 7 min. This extensive phase of activity ceased with the start of the flank effusive activity, which started on 2 April and continued through 7 April 2007. From the middle of February until around middle of April, data recorded from the SVO strainmeter show the highest strain rate during the year that high strain rate corresponded to the increase of the Strombolian activity. The extensive activity was not preceded by an increase of seismicity and only the largest explosion on 15 March shows clearly, in the short period before the occurrence of this event, a change in strain rate, while the data recorded during the effusive phase on 27 February show a decrease in the strain rate ~2 hr after the lava flow.

Very interesting signals have been recorded during a more intense explosion, on 15 March 2007, which extruded massive lava blocks to >1 km distant from the active craters (Pistolesi et al., 2011). The data recorded at both strainmeters (see Figure S0 in the supporting information) indicate that

a. before the explosion

   1. for ~660 s before, there is a slow source pressure buildup (green background in Figure S0);
   2. for 45 s, source pressure does not increase or decrease but exhibits an 8 s oscillation: this Observation suggests that the conduit is still sealed (yellow background in Figure S0);

b. after the explosion:

   1. there is a 20 s period with decaying oscillations, mainly due to gas emissions (orange background in Figure S0);
   2. pressure and strain observations indicate an oscillation in the air lasting 1,100 s at SVO and 800 s at TDF: This effect is driven by the collapse of the eruptive column, creating a gravitational load on the volcanic edifice.

2.2. The 2019 Paroxysms

2.2.1. The 3 July Event

During the weeks and months preceding the paroxysmal eruption on 3 July 2019, no significant changes in the strain and other monitored volcanic parameters were observed. During the period from December 2018 to January 2019, the volcano had a phase of higher activity, followed by an activity level classified as “low to moderate.” The activity increased from June 2019, keeping a “moderate” level from 12 June until the day before the eruption. This kind of behavior in volcano dynamics has been very common in recent years.

Almost 1 hr before the paroxysm, at 3:59 p.m. on 3 July, a new vent appeared on the upper break in slope of the Sciara del Fuoco (SdF), a few 100 m northwest from the crater terrace: Hot rocks broke off and, shortly after, a small lava flow started and slowly traveled downslope (retrieved from http://www.ingv.it/it/stampa-e-urp/stampa/comunicati-stampa-1/2019/37-comunicato-straordinario-stromboli-04-07-2019-09-00-utc-aggiornamento-sul-fenomeno-in-corso/file). The appearance of this new vent was the only precursor so far known: The magma in the conduit was experiencing a pressure rise from underneath and opened a small side-wise vent. Immediately before the onset of the paroxysm, lava flows emerged from all vents. The speed of the magma being pushed out from the conduit dramatically increased along with seismic activity which, then, quickly started to increase. One minute later, an extremely large gas bubble arrived at the surface and generated two lateral blasts (as reported by INGV in surveillance camera videos—see www.ingv.it) and a few seconds later the paroxysmal explosion started. In the time-lapse videos recorded by INGV thermal cameras, the giant lava bubble bursting out from the crater is clearly visible. Most of the summit area was then under rain of lava bombs of all sizes.

2.2.2. The 28 August Event

This paroxysmal event produced an eruptive column, which reached a height of 4 km above the crater summit. The paroxysm was preceded by an increase of the strombolian activity starting a day before. On 28 August, the paroxysmal sequence began, consisting of three explosive events, two of which were located in the central-southern crater area, while the third—the least energetic of the sequence—occurred 20 s later in the northern area, causing a lateral blast whose products spilled out over the SdF. The products generated by the collapse of the eruption plume, as well as those produced by the lateral blast, contributed to the

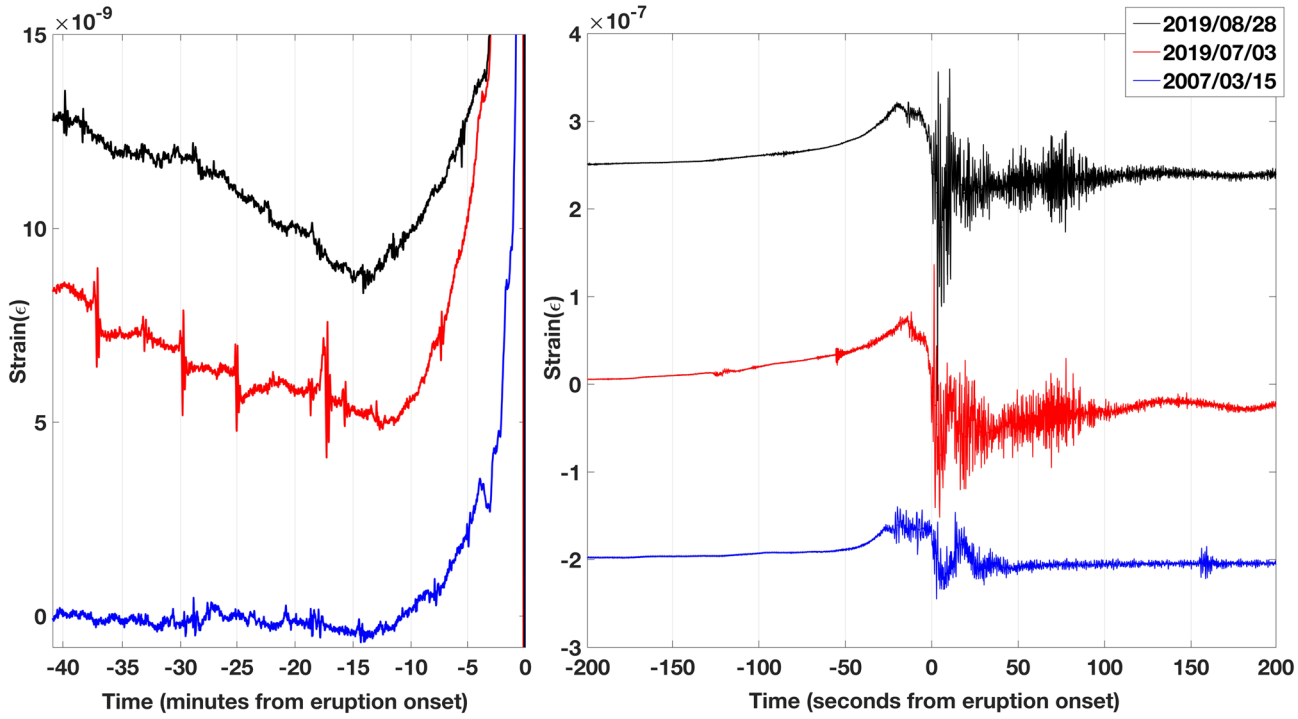

Figure 2. Comparison of strainmeter signals (contraction positive) observed at SVO during 2007 (blue line), July (red line) and August 2019 (black line) paroxysmal eruptions. Figure S2a shows that the change in strain starts 10 to 15 min before the events. Figure S2b shows that the two 2019 explosions are quite similar and larger than the 2007 event. Earth tides and atmospheric pressure are removed. A high pass filter (for periods shorter than 5,000 s) has been applied.

generation of a pyroclastic flow: it traveled down the SdF, reached the sea level and traveled several hundred meters out to sea. The full explosive sequence produced several morphological modifications of the northern area of the crater terrace overlooking the SdF (see for further descriptions INGV website).

3. Data Interpretation

The 2007 source pressure variations have been related to overpressurization and depressurization of a shallow magmatic chamber, located at 1.5 km depth, responsible for the vulcanian blast (Bonaccorso et al., 2012). On Mt. Stromboli, a detailed analysis of volcanic tremor leads to the hypothesis of nonlinear coupling of gas fluctuations within surrounding rocks as the main source of observed wavefield and other signal features of volcanic tremor during the steady state behavior of the volcano (De Lauro et al., 2008). The dilatometer data (Figure S0) reveal that the process of pressurization of the conduit starts about 11 min before the explosion, as indicated by the microbarograph signal.

Initially, there is an inflation at SVO, whereas TDF strain change has the opposite sign. This observation has been modeled in terms of a source inflation located at about 1.5 km depth, just before and following the explosion (Bonaccorso et al., 2012). Then, some minutes later, we observe contraction at both stations, corresponding to a shallower source, linked to a gas-magma slug along the upper portion of the conduit. The 20 s oscillations of strain after the explosion are similar to the observations made by Chen et al. (2018) at Montserrat volcano, suggesting an interaction between a shallow and a deeper magma chamber.

After the paroxysm occurred in 2007, Stromboli entered a new phase, characterized by persistent activity, sometimes accompanied by major explosions and/or overflow of lava from the summit craters. This phase culminated in an increase of the most energetic episodes, which led to an effusive eruption in August 2014 and a major eruption in October of the same year (Di Traglia et al., 2018). These events, although significant, have not been analyzed in the current paper because no data were available from the strainmeters.

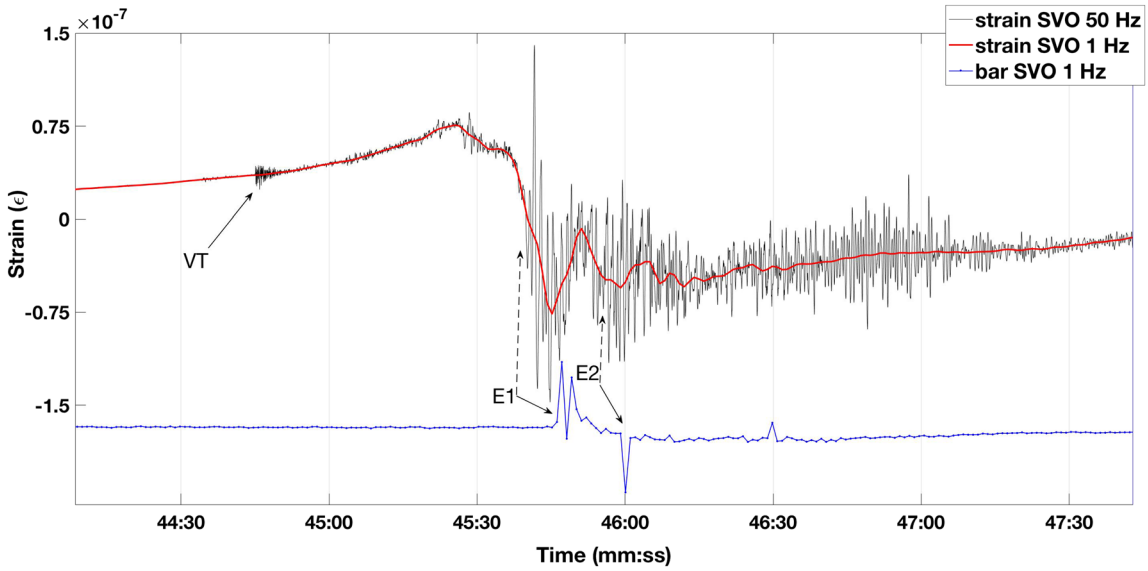

Figure 3. Strain (contraction positive) observed at SVO during the 3 July 2019 paroxysm. Red and black lines represent low sampled channel (1 sps) and high frequency sampled channel (50 sps), respectively, while the blue line shows the microbarograph signal. Tides have been removed. The occurrence of the volcano-tectonic (VT) event is indicated. The dashed arrow indicates the timing of the first explosion (E1) and, 6 s later, the pulse in the barograph record. A second explosion (E2) shows clearly in the microbarograph signal. Also, in this case, the dashed arrow indicates the most likely strain value corresponding to the onset of the second explosion.

The strainmeter signals recorded before, during, and after the paroxysmal activity of 3 July 2019 are surprisingly similar to the 2007 event but larger in amplitude and time duration (Figure 2). Due to malfunctioning of the recording system TDF, only records from the site SVO are available. The strain signal however shows a slow strain increase clearly evident at least 10 min before the explosion. During this build up, a VT event occurred, presumably triggered by the strain increase, as evident from the high frequency dilatometer signal. Two explosions correlate with two sudden strain drops and with the subsequent high frequency signals due to air shock and related air pressure fluctuations (E1 and E2 in Figure 3). The first air pressure pulse has been used as marker of the eruption onset, considering the delay time (almost 6 s from the main vent of the crater

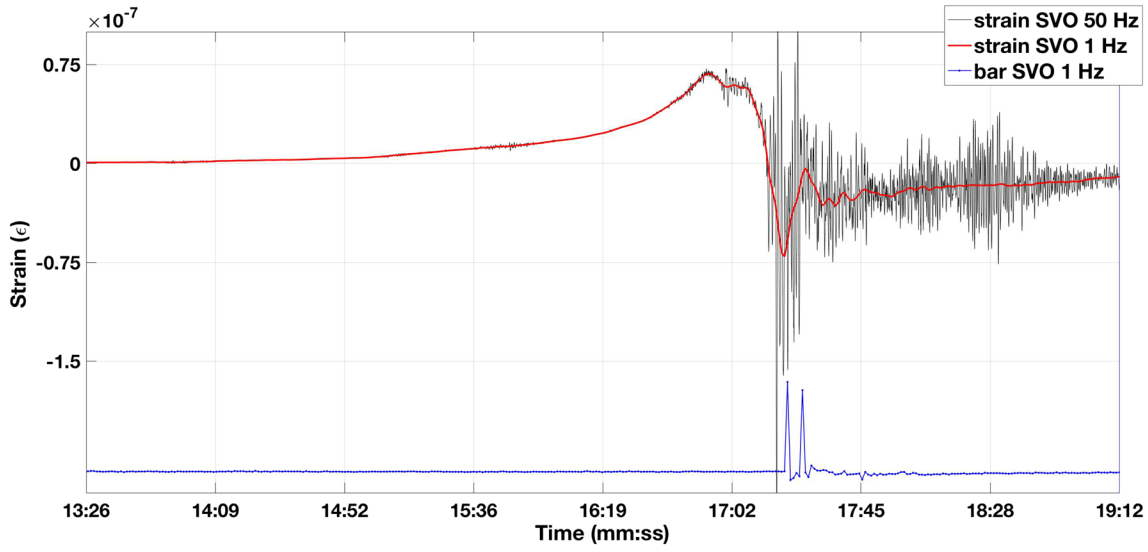

Figure 4. Strain (contraction positive) observed at SVO during the 28 August 2019 paroxysm. Red and black lines represent low sampled channel (1 sps) and high frequency sampled channel (50 sps), respectively, while the blue line shows the microbarograph signal. Tides have been removed.

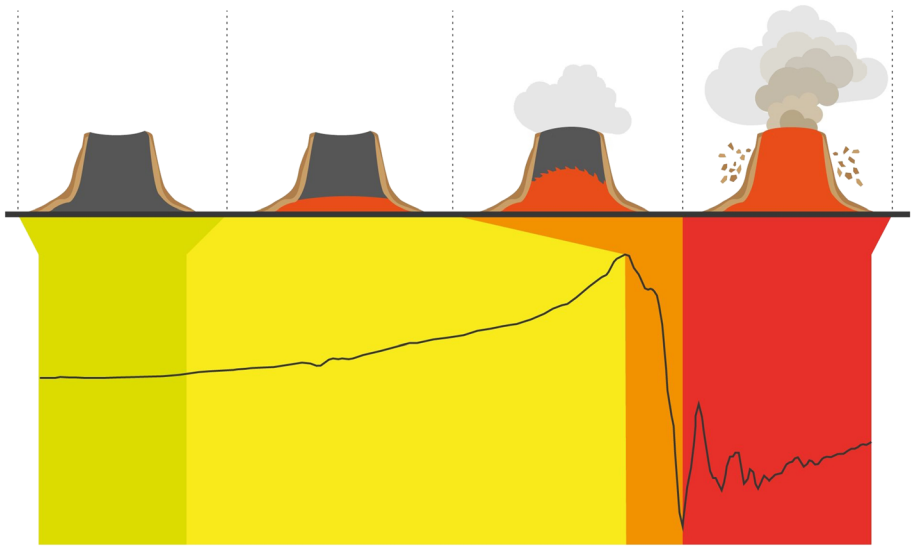

Figure 5. Schematic plot of the 2007 and 2019 paroxysm mechanism. The black line evidences the strain signal recorded corresponding to the main phases of gas-magma ascent. Green indicates the preparoxysm period. No particular changes of the signals or in the usual activity have been noticed. Yellow shows the pressure accumulation in the upper chamber. This phase lasts about 10 min. Orange shows the depressurization activity linked to the initial phase of the paroxysm and red the last phase associated to the blast, to the air shock and to refilling from a deeper magma chamber.

to the barometer installed at the SVO site) due to the speed of propagation of the air wave: 15 s pass between the beginning of the stress drop and the shock wave arrival. After 30 min, the strain reverts to the preeruptive level, showing the end of activity, with very long period oscillations. For both paroxysms, corresponding to a Volcanic Explosivity Index (VEI) = 2, there was an increase of degassing (visible from the enhanced tremor) just after the explosions. Strainmeter signals show that the size of the July 2019 explosion is larger by a factor of 3 than the 2007 event. The ash column associated with this explosion extended to 5 km above the craters.

The strain recorded at SVO strainmeter shows many features similar to the 3 July event. The overall strain pattern looks very similar to the one recorded during the previous paroxysm, showing a very slow strain buildup, which becomes clearly observable several minutes before the explosion. Two major explosions are visible from the air pressure data, occurring soon after the decrease of the strain (Figure 4). As for the two previous paroxysms from 2007 and earlier in 2019, the strain pattern shows an abrupt depressurization starting about 21 s before the air shock wave—defining the beginning of the paroxysm—that is recorded by the barometer installed near the strainmeter.

4. Discussion

Stromboli eruptions shows many similarities with Sakurajima vulcanian eruptions, where a cyclic inflation-deflation pattern of ground deformation has been associated with each eruption (Iguchi et al., 2008). This cycle is used to forecast eruptions, as an inflationary radial tilt is observed for periods of 10 min to 7 hr prior to eruptions, enabling automated warnings to be issued (Kamo & Ishihara, 1989). The complexity of the magma feeding system, due to the presence of multiple vents at the surface, does allow a reliability of the eruption prediction scheme only at a confidence level of 70%. The gas leakage phenomena introduce further mechanisms, providing a more complicated pattern of precursors (Yokoo et al., 2013).

As related to the mechanisms of the paroxysmal activity of Stromboli, a general model for the dynamics of paroxysmal explosions at Stromboli is not yet available and remains a matter of debate. Since the magma plumbing system of the Stromboli volcano is widely studied from geophysical, vulcanological, and geochemical perspectives, it has been recognized that the feeding system can be depicted as a vertical column (see, e.g., Métrich et al., 2010), connecting the open vents on the surface with a shallow ponding zone located at 2–4 km bsl (Bonaccorso et al., 2012). The deeper reservoir is located at 7–10 km depth (Morelli et al., 1975; Ubide et al., 2019): It is now widely recognized that these deep, low porphyricity

magma reservoirs play an important role in triggering paroxysmal activity. These eruptions are triggered by a larger supply of deep magma or gas-magma as demonstrated from the petrological analysis of products of the 1930 and XVI century eruptions (Bertagnini et al., 2011). The mechanism proposed by Calvari et al. (2011) suggests instead that the triggering is generated by the emptying of the upper part of the conduit due to prolonged lava activity. This process is based on the daily measurements of effusive activity and from the consideration that the threshold in the decompression rate is proportional to the height of the bubbly LP magma, as evident for the 2002 and 2007 activity. Unlike that of 2007, the last eruptions of 2019 were not preceded by lava emission activity during the months preceding the paroxysm but only by overflow in the upper part of the conduits just a few minutes before the explosion. It is likely that the triggering mechanism for the 2019 paroxysms is the enhanced flux of magma, different from the 2007 paroxysm which is complicated by the lava flux, as evident from the simple strain rate signals observed for the 2019 activity as compared to the many short-period oscillations of the strain before the starting of 2007 blast (Figures S0 in the supporting information and 2).

It has already been shown, from the strain data recorded during the 2007 vulcanian activity by Bonaccorso et al. (2012), the strain field changes at $r = \sqrt{2}d$ where r is the radial distance and d is the source depth, as a result of the Mogi model. The source depth d has been found at Stromboli to be at 1.4 km bsl, which is realistic also for 2019 sources due to the comparable size of these two explosions. By using the simple source model proposed by McTigue (1987), the observed strain during the 2019 events can be simply attributed to a source located at 1.4 km depth with volume loss amounting to 10^6 m^3, which is comparable with the ejected volume of tephra. This approach is very simple and this depth may be considered also as a lower limit value.

The duration of the signals and the rate of strain build up and drop are compatible with a gas-magma recharge rate of $\approx 10^3$ m^3/s from a shallow reservoir. Pistolesi et al. (2011) estimated a comparable value for the 2007 paroxysm. The 20 s strain oscillations soon after the paroxysms are probably related to magma ascent fluctuations from a shallower source, located in the upper portion of the magma conduits. The cyclic strain changes can be interpreted as induced by the forced flow of melt and the magmatic fluids into a narrow dike which form the upper magma conduit. The values of the oscillations during the vulcanian explosions are compatible with a source of size of 200 meters. In the supporting information, there is a more detailed discussion on the approach to derive these last parameters in analogy with the longer period oscillations (20 min) recorded at SHV, Montserrat, modeled by Chen et al., (2018).

A schematic of the mechanism for the 2019 paroxysms is illustrated in Figure 5, in which the normal volcanic activity (preparoxysmal phase) is shown in green. The yellow phase can be interpreted as the pressure growth in the upper chamber due to the accumulation of the gas-magma slug. In this phase, strain builds up, until a threshold value is reached. From the time-lapse video published on the INGV website, it is possible to verify that once the maximum value of the strain is reached, all the crater vents start a more vigorous degassing phase, concurrently with the stress drop recorded by the strainmeter and depicted in orange in Figure 5: This is a usual habit for other open conduit volcanoes, like Sakurajima in Japan (Kazahaya et al., 2016). The final, red phase, occurs once the paroxysm begins: higher frequencies are observed as a consequence of the complex activity occurring in the summit craters area. This activity is very similar to the 1930 blast, as suggested by Bertagnini et al. (2011), which is the largest explosive eruption of the twentieth century at Stromboli. The 2007 mechanism is more complicated by the presence of the higher decompression rate due to the lava flow.

5. Conclusions

The installed borehole strainmeters contribute to the knowledge of the magma feeding system and deformation mechanism at Stromboli.

The high resolution of deformational changes in the subsurface allows borehole strainmeters uniquely to resolve signals that are typically invisible to other geodetic/geophysical monitoring instruments. Numerous studies on borehole strainmeter records from active volcanoes worldwide contributed already significantly toward (i) the detailed resolution of complex magmatic systems in the subsurface (Hautmann et al., 2013; Linde et al., 2016), (ii) the understanding of long-term (Hautmann et al., 2017) and short-term eruption dynamics (Hautmann et al., 2014), and (iii) the identification of early warning signals preceding

the onset of eruptive events (Bonaccorso et al., 2014; Sturkell et al., 2013). Our study presented adds to this list, as we show three cases of high quality strain signals and some relatively long period oscillations, during the explosions, which help in putting constraints on the size of conduits. In addition, the analyzed data are of high value for early warning purposes, as the records unveil for the first time a distinct pressure increase over 15 min preceding discrete, short-term explosion events at Stromboli. An early warning system for civil protection will be implemented in future by using these signals and transmitting in real-time variable alert levels (see also Giudicepietro et al., 2020). Further contribution for a better and more quantitative interpretation of these data will be derived from the planned installation of an additional borehole strainmeter and a two long baseline high sensitivity tiltmeters and by the inclusion in the data base of all the geophysical and geochemical data collected by the present monitoring networks.

Data Availability Statement

Data used in the current paper have been submitted to the PANGAEA—Data Publisher for Earth and Environmental Science repository: Romano, Pierdomenico; Di Lieto, Bellina; Scarpa, Roberto; Linde, Alan T. (2020): Paroxysm-induced early warning signals at Stromboli volcano, Italy. PANGAEA (https://doi.org/10.1594/PANGAEA.913495)

Acknowledgments
This study was supported by Istituto Nazionale di Geofisica e Vulcanologia and by Italian Civil Protection Department. It received financial support from the Italian Department of Civil Protection. The authors would like to thank Stefanie Hautmann and the other anonymous reviewer who, with their suggestions, considerably helped with improving this manuscript and A. Paraggio who provided the image of the eruptive mechanism.

References

Bertagnini, A., Di Roberto, A., & Pompilio, M. (2011). Paroxysmal activity at Stromboli: Lessons from the past. *Bulletin of Volcanology*, *73*, 1229–1243. https://doi.org/10.1007/s00445-011-0470-3

Bonaccorso, A., Calvari, S., Linde, A., & Sacks, S. (2014). Eruptive processes leading to the most explosive lava fountain at Etna volcano: The 23 November 2013 episode. *Geophysical Research Letters*, *41*, 4912–4919. https://doi.org/10.1002/2014GL060623

Bonaccorso, S., Calvari, S., Linde, A., Sacks, S., & Boschi, E. (2012). Dynamics of the shallow plumbing system investigated from borehole strainmeters and cameras during the 15 March, 2007 vulcanian paroxysm at Stromboli Volcano. *Earth and Planetary Science Letters*, *357–358*, 249–256. https://doi.org/10.1016/j.epsl.2012.09.009

Calvari, S., Spampinato, L., Bonaccorso, A., Oppenheimer, C., Rivalta, E., & Boschi, E. (2011). Lava effusion—A slow fuse for paroxysms at Stromboli volcano? *Earth and Planetary Science Letters*, *301*, 317–323. https://doi.org/10.1016/j.epsl.2010.11.015

Chen, C.-W., Huang, H.-F., Hautmann, S., Sacks, I. S., Linde, A. T., & Taira, T. (2018). Resonance oscillations of the Soufrière Hills Volcano (Montserrat, W.I.) magmatic system induced by forced magma flow from the reservoir into the upper plumbing dike. *Journal of Volcanology and Geothermal Research*, *350*, 7–17. https://doi.org/10.1016/j.jvolgeores.2017.11.020

Chouet, B., Dawson, P., Ohminato, T., Martini, M., Saccorotti, G., Giudicepietro, F., et al. (2003). Source mechanism of explosions at Stromboli Volcano, Italy, determined from moment-tensor inversions of very-long-period data. *Journal of Geophysical Research*, *108*(B1), 2019. https://doi.org/10.1029/2002JB001919

Chouet, B., Saccorotti, G., Dawson, P., Martini, M., Scarpa, R., De Luca, G., et al. (1999). Broadband measurements of the sources of explosions at Stromboli Volcano, Italy. *Geophysical Research Letters*, *26*(13), 1937–1940. https://doi.org/10.1029/1999GL900400

Chouet, B., Saccorotti, G., Martini, M., Dawson, P., De Luca, G., Milana, G., & Scarpa, R. (1997). Source and path effects in the wavefields of tremor and explosions at Stromboli Volcano, Italy. *Journal of Geophysical Research*, *102*, 15,129–15,150. https://doi.org/10.1029/97JB00953

De Lauro, E., De Martino, S., Del Pezzo, E., Falanga, M., Palo, M., & Scarpa, R. (2008). Model for high-frequency Strombolian tremor inferred by wavefield decomposition and reconstruction of asymptotic dynamics. *Journal of Geophysical Research*, *113*, B02302. https://doi.org/10.1029/2006JB004838

De Lauro, E., De Martino, S., Falanga, M., Palo, M., & Scarpa, R. (2005). Evidence of VLP volcanic tremor in the band [0.2–0.5] Hz at Stromboli Volcano, Italy. *Geophysical Research Letters*, *32*, L17303. https://doi.org/10.1029/2005GL023466

De Martino, S., Falanga, M., Scarpa, R., & Godano, C. (2005). Very long period volcanic tremor at Stromboli Volcano, Italy. *Bulletin of the Seismological Society of America*, *95*(3), 1186–1192. https://doi.org/10.1785/0120040063

Di Traglia, F., Calvari, S., D'Auria, L., Nolesini, T., Bonaccorso, A., Fornaciai, A., et al. (2018). The 2014 effusive eruption at Stromboli: New insights from in situ and remote-sensing measurements. *Remote Sensing*, *10*, 2035. https://doi.org/10.3390/rs10122035

Giudicepietro, F., López, C., Macedonio, G., Alparone, S., Bianco, F., Calvari, S., et al. (2020). Geophysical precursors of the July–August 2019 paroxysmal eruptive phase and their implications for Stromboli volcano (Italy) monitoring. *Scientific Reports, 10,* 10296. https://doi.org/10.1038/s41598-020-67220-1

Hart, R. H. G., Gladwin, M. T., Gwyther, R. L., Agnew, D. C., & Wyatt, F. K. (1996). Tidal calibration of borehole strain meters: Removing the effect of small-scale inhomogeneity. *Journal of Geophysical Research*, *101*(B11), 25,553–25,571. https://doi.org/10.1029/96JB02273

Hautmann, S., Hidayat, D., Fournier, N., Linde, A. T., Sacks, I. S., & Williams, C. P. (2013). Pressure changes in the magmatic system during the December 2008/January 2009 extrusion event at Soufrière Hills volcano, Montserrat (W.I.), derived from strain data analysis. *Journal of Volcanology and Geothermal Research*, *250*, 34–41. https://doi.org/10.1016/j.jvolgeores.2012.10.006

Hautmann, S., Sacks, I. S., Linde, A. T., & Roberts, M. J. (2017). Magma buoyancy and volatile ascent driving autocyclic eruptivity at Hekla volcano (Iceland). *Geochemistry, Geophysics, Geosystems*, *18*, 3517–3529. https://doi.org/10.1002/2017GC007061

Hautmann, S., Witham, F., Christopher, T., Cole, P., Linde, A. T., Sacks, I. S., & Sparks, S. J. (2014). Strain field analysis on Montserrat (W.I.) as tool for assessing permeable flow paths in the magmatic system of Soufrière Hills volcano. *Geochemistry Geophysics Geosystems*, *15*, 676–690. http://doi.org/10.1002/2013GC005087

Iguchi, M., Yakiwara, H., Tameguri, T., Hendrasto, M., & Hirabayashi, J. (2008). Mechanism of explosive eruption revealed by geophysical observations at the Sakurajima, Suwanosejima and Semeru volcanoes. *Journal of Volcanology and Geothermal Research*, *178*(1), 1–9. https://doi.org/10.1016/j.jvolgeores.2007.10.010

Kamo, K., & Ishihara, K. (1989). A preliminary experiment on automated judgement of the stages of eruptive activity using tiltmeter records at Sakurajima, Japan. In J. H. Latter (Ed.), *Volcanic Hazards. IAVCEI Proceedings in Volcanology* (Vol. 1, pp. 585–598). Berlin, Heidelberg: Springer. https://doi.org/10.1007/978-3-642-73759-6_35

Kazahaya, R., Shinohara, H., Mori, T., Iguchi, M., & Yokoo, A. (2016). Pre-eruptive inflation caused by gas accumulation: Insight from detailed gas flux variation at Sakurajima volcano, Japan. *Geophysical Research Letters*, *43*, 11,219–11,225. https://doi.org/10.1002/2016GL070727

Linde, A. T., Kamigaichi, O., Churei, M., Kanjo, K., & Sacks, I. S. (2016). Magma chamber recharging and tectonic influence on reservoirs: The 1986 eruption of Izu-Oshima. *Journal of Volcanology and Geothermal Research*, *311*, 72–78. https://doi.org/10.1016/j.jvolgeores.2016.01.001

McTigue, D. F. (1987). Elastic stress and deformation near a finite spherical magma body: Resolution of the point source paradox. *Journal of Geophysical Research*, *92*, 12,931–12,940. https://doi.org/10.1029/JB092iB12p12931

Métrich, N., Bertagnini, A., & Di Muro, A. (2010). Conditions of magma storage, degassing and ascent at Stromboli: New insights into the volcano plumbing system with inferences on the eruptive dynamics. *Journal of Petrology*, *51*(3), 603–626. https://doi.org/10.1093/petrology/egp083

Morelli, C., Giese, P., Cassinis, R., Colombi, B., Guerra, I., Luongo, G., et al. (1975). Crustal structure of southern Italy. A seismic refraction profile between Puglia-Calabria-Sicily. *Bollettino Di Geofisica Teorica E Applicata*, *17*, 183–210.

Pistolesi, M., Delle Donne, D., Pioli, L., Rosi, M., & Ripepe, M. (2011). The 15 March 2007 explosive crisis at Stromboli volcano, Italy: Assessing physical parameters through a multidisciplinary approach. *Journal of Geophysical Research*, *116*, B12206. https://doi.org/10.1029/2011JB008527

Sturkell, E., Ágústsson, K., Linde, A. T., Sacks, S. I., Einarsson, P., Sigmundsson, F., et al. (2013). New insights into volcanic activity from strain and other deformation data for the Hekla 2000 eruption. *Journal of Volcanology and Geothermal Research*, *256*, 78–86. https://doi.org/10.1016/j.jvolgeores.2013.02.001

Ubide, T., Caulfield, J., Brandt, C., Bussweiler, Y., Mollo, S., Di Stefano, F., et al. (2019). Deep magma storage revealed by multi-method elemental mapping of clinopyroxene megacrysts at Stromboli Volcano. *Frontiers in Earth Science*, *7*, 239. https://doi.org/10.3389/feart.2019.00239

Yokoo, A., Iguchi, M., Tameguri, T., & Yamamoto, K. (2013). Processes prior to outbursts of vulcanian eruption at Showa crater of Sakurajima volcano. *Bulletin of Volcanological Society of Japan*, *58*(1), 163–181. https://doi.org/10.18940/kazan.58.1_163

References From the Supporting Information

Davis, P. M. (1986). Surface deformation due to inflation of an arbitrarily oriented triaxial ellipsoidal cavity in an elastic half-space, with reference to Kilauea volcano, Hawaii. *Journal of Geophysical Research*, *91*, 7429–7438. https://doi.org/10.1029/JB091iB07p07429

Roeloffs, E. A., & Linde, A. T. (2007). Borehole observations of continuous strain and fluid pressure. In *Volcano deformation. Springer praxis books* (pp. 305–322). Berlin, Heidelberg: Springer. https://doi.org/10.1007/978-3-540-49302-0_9